

Multi-level Compositional Feature Augmentation for Unbiased Scene Graph Generation

Lin Li*, Xingchen Li*, Chong Sun, Chen Li, and Long Chen[✉]

Received: date / Accepted: date

Abstract Scene Graph Generation (SGG) aims to detect all the visual relation triplets $\langle \text{sub}, \text{pred}, \text{obj} \rangle$ in a given image. With the emergence of various advanced techniques for better utilizing both the intrinsic and extrinsic information in each relation triplet, SGG has achieved great progress over the recent years. However, due to the ubiquitous long-tailed predicate distributions, today's SGG models are still easily biased to the head predicates. Currently, the most prevalent debiasing solutions for SGG are re-balancing methods, *e.g.*, changing the distributions of original training samples. In this paper, we argue that all existing re-balancing strategies fail to increase the diversity of the relation triplet features of each predicate, which is critical for robust SGG. To this end, we propose a novel **Multi-level Compositional Feature Augmentation (MCFA)** strategy, which aims to mitigate the bias issue from the perspective of increasing the diversity of triplet features. Specifi-

Lin Li
 Department of Computer Science and Engineering
 The Hong Kong University of Science and Technology, Hong Kong
 E-mail: illidy@ust.hk

Xingchen Li
 China Mobile (Zhejiang) Research & Innovation Institute
 E-mail: xingchenl@zju.edu.cn

Chong Sun
 Tencent
 E-mail: waynecsun@tencent.com

Chen Li
 Tencent
 E-mail: chaselli@tencent.com

Long Chen
 Department of Computer Science and Engineering
 The Hong Kong University of Science and Technology, Hong Kong
 E-mail: longchen@ust.hk

* Equal contribution.

[✉]Long Chen is the corresponding author.

cally, we enhance relationship diversity on not only *feature-level*, *i.e.*, replacing the intrinsic or extrinsic visual features of triplets with other correlated samples to create novel feature compositions for tail predicates, but also *image-level*, *i.e.*, manipulating the image to generate brand new visual appearance for triplets.

Due to its model-agnostic nature, MCFA can be seamlessly incorporated into various SGG frameworks. Extensive ablations have shown that MCFA achieves a new state-of-the-art performance on the trade-off between different metrics.

Keywords Unbiased Scene Graph Generation · Feature Augmentation · Category Clustering · Compositional Learning

1 Introduction

As one of the fundamental comprehensive visual scene understanding tasks, Scene Graph Generation (**SGG**) has attracted unprecedented interest from our community and has made great progress in recent years [29, 45, 43, 2, 3, 36, 23, 19]. Specifically, SGG aims to transform an image into a visually-grounded graph representation (*i.e.*, scene graph) where each node represents an object instance with a bounding box and each directed edge represents the corresponding predicate between the two objects. Thus, each scene graph can also be formulated as a set of visual relation triplets (*i.e.*, $\langle \text{sub}, \text{pred}, \text{obj} \rangle$). Since such structural representations can provide strong explainable potentials, SGG has been widely-used in various downstream tasks, such as visual question answering, image retrieval, and captioning.

In general, due to the extremely diverse visual appearance of different visual relation triplets, recent SGG methods all consider both *intrinsic* and *extrinsic* information for entity and predicate classification [43, 35, 30].

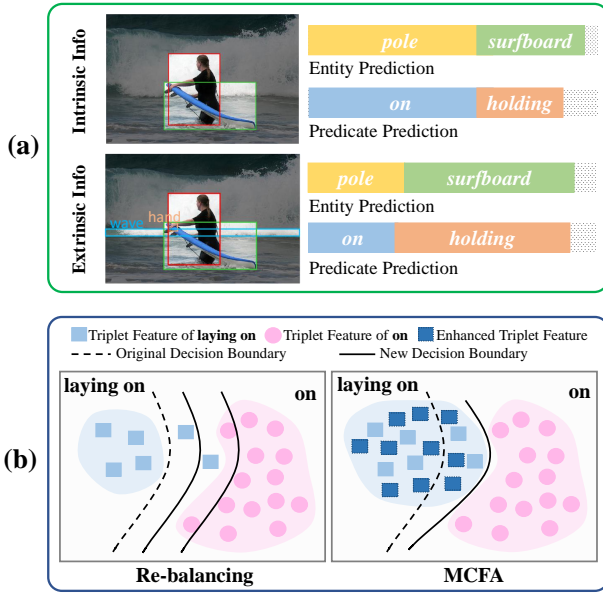
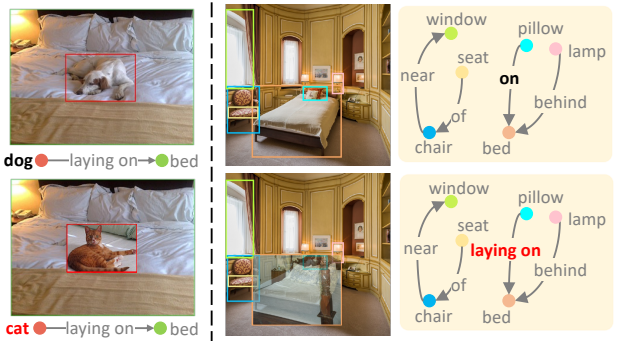


Fig. 1: (a) The intrinsic and extrinsic information for SGG. The entity prediction is for the green box, and the predicate prediction is for the relation between the red and green boxes. (b) Illustration of the diversity of feature space and decision boundary between on and laying on before and after using re-balancing and MCFA. Each sample denotes the corresponding visual triplet features.

By “intrinsic information”, we mean these intrinsic characteristics of the subjects and objects, such as their visual, semantic, and spatial features. For example in Fig. 1(a), with the help of these intrinsic features, we can easily infer all possible entity categories (*e.g.*, pole or surfboard) and predicate categories (*e.g.*, on or holding) of each triplet. However, sometimes it is still hard to confirm the exact correct predictions with only intrinsic information, especially for tiny objects. Thus, it is also essential to consider other “extrinsic information” in the same image, such as the context features from neighbor objects. As shown in Fig. 1(a), after encoding the features of surrounding objects (*e.g.*, wave and hand), we can easily infer that the categories of the entity and predicate should be surfboard and holding.

Although numerous advanced techniques have been proposed to enhance SGG performance. Today’s SGG methods still fail to predict some informative predicates due to the ubiquitous long-tailed predicate distribution in prevalent SGG datasets [18]. Such a distribution is characterized by a small amount categories with vast samples (head¹) and plenty of categories with rare samples (tail). As a result of the discrepancy of sample size among different cat-

¹We directly use “tail”, “body”, and “head” categories to represent the predicate categories in the tail, body, and head parts of the number distributions of different predicates in SGG datasets, respectively.



(a) Intrinsic-CFA

(b) Extrinsic-CFA

Fig. 2: (a) Intrinsic-CFA: Replacing the entity feature of tail predicate triplet dog-laying on-bed from dog to cat to enhance the intrinsic feature. (b) Extrinsic-CFA: Mixing up the feature of tail predicate triplet pillow-laying on-bed into the context of pillow-on-bed to enhance the extrinsic feature.

egories, the learned decision boundary becomes improper (*cf.* Fig. 1(b)), *i.e.*, their predictions are biased towards the head predicates (*e.g.*, on) and they are error-prone for the tail ones (*e.g.*, laying on).

To overcome the bias issue, the most prevalent unbiased SGG solutions are re-balancing strategies, *e.g.*, sample re-sampling [23] and loss re-weighting [41, 1, 24, 31]. They alleviate the negative impact of long-tailed distribution by increasing samples or loss weights of tail classes. Then, the decision boundaries are adjusted to reduce the bias introduced by imbalanced distributions. However, we argue that all the existing re-balancing strategies only change the frequencies or contributions of existing relation triplets to improve the skewed decision boundaries, but fail to enhance the diversity of *relation triplet features*² of each predicate, which is crucial to infer their complete feature space. This sparsity of feature diversity will lead to under-representation of tail categories, thereby making it hard to infer the complete data distribution, *i.e.*, making it challenging to find the optimal direction to adjust the decision boundaries [6, 38]. For example in Fig. 1(b), the feature space of laying on is so sparse that the decision boundary can be adjusted within a large range. The performance of this naive adjustment without “complete” distribution is always sensitive to hyperparameters, *i.e.*, excessively increasing the sample number or loss weight of tail predicates may cause some head predicate samples to be incorrectly predicted as tail classes (right solid line), and vice versa (left solid line).

Therefore, in this paper, we focus on *enhancing diversity of relation triplet features* instead of re-balancing their frequencies to learn more robust feature space and decision boundaries for predicates. One intuitive idea is to borrow

²We use the “relation triplet feature” to represent the combination of both **intrinsic** and **extrinsic** features of each visual relation triplet.

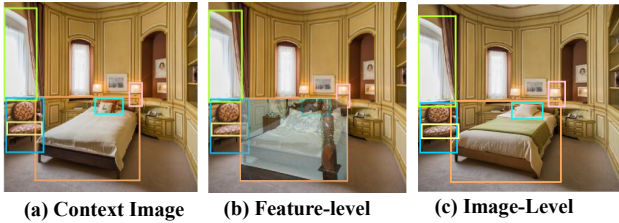


Fig. 3: (a) **Context Image**: The image which provides context information and is used to augment with the triplet `pillow-on-bed`. (b) **Feature-level Augmentation**: Visualization of augmented results with the feature of tail predicate triplet `pillow-laying on-bed` selected from dataset. (c) **Image-level Augmentation**: Augmented new image with target triplet and context information by generative models.

novel entity features or context features from other existing triplet samples to replace the original features, thereby constructing new triplet features for the target predicates. By deeply exploring the correlations of objects and predicates, we can reasonably select the features to replace, ensuring the reliability of the re-composed relation triplet features. However, this naive augmentation technique on *feature-level* manipulation has its inevitable limitations. On the one hand, directly replacing the original visual features may lead to unnatural transitions (*e.g.*, fusing a pillow’s feature with another one that are inadvertently entangled with adjacent objects, such as bedside cupboard) as shown in Fig. 3(b), further hurting the expressive ability of the model. On the other hand, the augmented samples are still limited to the in-domain distribution, and as a result, the trained models are unable to handle with out-of-domain predictions. Therefore, we also propose to manipulate relation triplet features on *image-level* with the help of powerful generative models as shown in Fig. 3(c).

In this paper, we propose a novel Multi-level Compositional Feature Augmentation (MCFA) strategy for unbiased SGG, which tries to solve the bias issue by enhancing the diversity of relation triplet features on both *feature-level* and *image-level*, especially for tail predicates.

As shown in Fig. 1(b), by enhancing the feature diversity of the tail predicates (*e.g.*, `laying on`), SGG models can easily learn the proper decision boundaries (vs. re-balancing strategies).

On **feature-level**, we apply different strategies for augmenting intrinsic and extrinsic feature diversity respectively. For **intrinsic diversity**, we replace the entity features (*e.g.*, subject or object) of a tail predicate triplet with other “suitable” entity features. To determine the suitable entity categories for the augmentation, we propose a novel *relation-conditioned entity clustering* method to find the predicate-aware correlations between different entity categories, and

then we regard the entity features from the same cluster are suitable. Specifically, we calculate the category correlation by pattern, context, and semantic similarities. For example in Fig. 2 (a), the entity categories `cat` and `dog` are in the same cluster, *i.e.*, we can augment the intrinsic feature by replacing the `dog` entity feature with a `cat` entity feature. For **extrinsic diversity**, we take advantage of the context or interactions of other triplets (*i.e.*, context triplets) and enhance the features of tail predicate triplets by these context triplets. Specifically, given a context triplet randomly selected from an image, we first select a reasonable tail predicate triplet as the target by limiting the categories and relative position of two objects. Then, to minimize the impact on the prediction of other triplets in the original image and make use of the extrinsic features of the context triplet, we use an *adaptive mixup strategy* to fuse the features of targeted tail predicate triplet into the context triplet and adaptively adjust mixup weights based on predicate semantic similarity. For example in Fig. 2 (b), triplet `pillow-laying on-bed` is mixed up into the image of `pillow-on-bed`. To avoid introducing noise into augmented samples, we adaptively assign weights to the mixed triplets by considering the semantic similarity of relation triplets.

On image-level, we aim to directly manipulate the images and generate brand-new visual appearances for target predicate triplets. A core challenge in this process is ensuring the semantic plausibility and spatial coherence of the generated images. To address this, we first employ a relative position constraint to filter only contextually appropriate images associated with target triplet categories for augmentation. For the synthesis process, we leverage the powerful grounded text-to-image generation capabilities of recent generative models (*e.g.*, GLIGEN [26]), as shown in Fig. 3(c). Specifically, the model is conditioned on the original image, the target triplet’s categories, and corresponding entity grounding information to generate a new high-quality visual instance. Subsequently, we assess the quality of each generated image via a visual-language similarity score to ensure high fidelity and relevance. As the context triplets are selected from other predicate triplets and visual features of target triplets are novelly generated, both **extrinsic** and **intrinsic diversity** are enhanced under our image-level augmentation strategy.

We evaluate MCFA on two most prevalent and challenging SGG datasets: Visual Genome (VG) [18] and GQA [15]. Since MCFA is a model-agnostic debiasing strategy, it can be seamlessly incorporated into various SGG architectures and consistently improve their performance. Unsurprisingly, MCFA can achieve a new state-of-the-art performance on the trade-off between different metrics. Extensive ablations and results on multiple SGG tasks and backbones have shown the generalization ability and effectiveness of MCFA.

This paper is a comprehensive and in-depth extension of our previous ICCV work [21] with several significant improvements:

1. We propose a novel relation-conditioned entity clustering strategy for feature-level intrinsic augmentation by leveraging the predicate-driven semantic knowledge, leading to more accurate groupings.
2. We propose an adaptive mix-up strategy for feature-level extrinsic augmentation, which dynamically adjust mix-up coefficient based on predicate similarity, effectively handling with the varying semantic context of triplets.
3. We devise a novel generative augmentation method to manipulate relation triplet features on the image-level and generate high-quality samples, thereby effectively boosting the performance of tail predicates.
4. Extensive qualitative and quantitative analyses demonstrate the effectiveness of our MCFA.

2 Related Work

Unbiased Scene Graph Generation. Biased predictions prevent further use of scene graphs in real-world applications. Recent unbiased SGG works can be divided into three main categories: 1) *Re-balancing*: It alleviates the negative impact of long-tailed predicate distribution by re-weighting or re-sampling [41, 24, 31, 23, 8]. 2) *Unbiased Inference*: It makes unbiased predictions based on biased models [36, 42]. 3) *Noisy Label Learning*: It reformulates SGG as a noisy label learning problem and corrects the noisy samples [19, 20]. This work points out the drawbacks of existing re-balancing methods and studies unbiased SGG from the new perspective of multi-level feature augmentation.

Feature Augmentation. Data augmentation is a prevalent training trick to improve models' performance. Conventional data augmentation methods [9, 46] usually synthesize new samples in a hand-crafted manner. Compared to these image-level data augmentation methods, feature augmentation is another efficient way to improve models' generalizability by directly synthesizing samples in the feature space [6, 22]. Compared to existing data augmentation applications, SGG is a sophisticated task that involves intrinsic and extrinsic features. In this work, we propose MCFA to enrich the diversity of relation triplet features for debiasing from both feature-level and image-level.

Compositional Learning (CL). CL has been successfully applied to various computer vision tasks. As for visual scene understanding, some Human Object Interaction (HOI) detection works [13, 17, 14] compose new interaction samples that significantly benefit both low-shot and zero-shot settings. Inspired by these successes, we adopt this compositional approach for unbiased SGG. Our method enhances triplet feature diversity by first decomposing representations

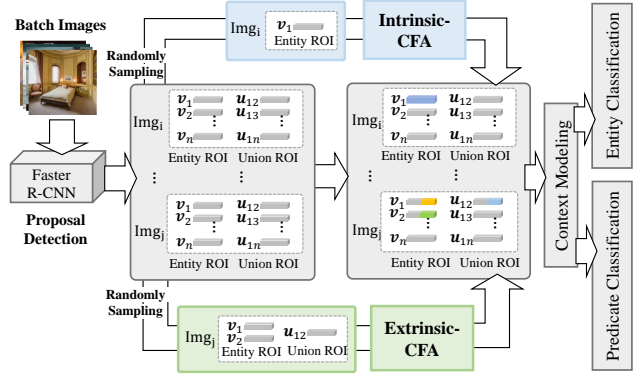


Fig. 4: The illustration of unbiased SGG framework with MCFA on feature-level augmentation.

into their intrinsic and extrinsic constituents, and then augmenting these two feature streams.

3 Multi-level Compositional Feature Augmentation

Given an image I , a scene graph is formally represented as $\mathcal{G} = \{\mathcal{N}, \mathcal{E}\}$, where \mathcal{N} and \mathcal{E} denote the set of all objects and their pairwise visual relations, respectively. Specifically, the i -th object in \mathcal{N} consists of a bounding box (bbox) $b_i \in \mathcal{B}$ and its entity category $o_i \in \mathcal{O}$. A relation $r_{ij} \in \mathcal{R}$ denotes the predicate category between i -th object and j -th object. b_{ij} denotes the union box of bbox b_i and bbox b_j . \mathcal{B} , \mathcal{O} , and \mathcal{R} represent the set of all entity bboxes, entity categories, and predicate categories, respectively.

In this section, we first revisit the two-stage SGG baselines in Sec. 3.1. Then, we elaborate the pipeline of MCFA, including feature-level and image-level feature augmentation strategy (cf., Fig. 4) in Sec. 3.2 and Sec. 3.3, respectively. Finally, we detail the training objectives in Sec. 3.4.

3.1 Revisiting the Two-Stage SGG Baselines

Since the mainstream SGG methods are two-stage models, we review the two-stage SGG framework here [43, 35]. A typical two-stage SGG model involves three steps: proposal generation, entity classification, and predicate classification. Thus, the SGG task $P(\mathcal{G}|I)$ is decomposed into:

$$P(\mathcal{G}|I) = P(\mathcal{B}|I)P(\mathcal{O}|\mathcal{B}, I)P(\mathcal{R}|\mathcal{O}, \mathcal{B}, I). \quad (1)$$

Proposal Generation $P(\mathcal{B}|I)$. This step aims to generate all bbox proposals \mathcal{B} . Given an image I , they first utilize an off-the-shelf object detector (e.g., Faster R-CNN [34]) to detect all the proposals \mathcal{B} and their visual features $\{\mathbf{v}_i\}$.

Entity Classification $P(\mathcal{O}|\mathcal{B}, I)$. This step mainly predicts the entity category of each $b_i \in \mathcal{B}$. Given a visual feature \mathbf{v}_i

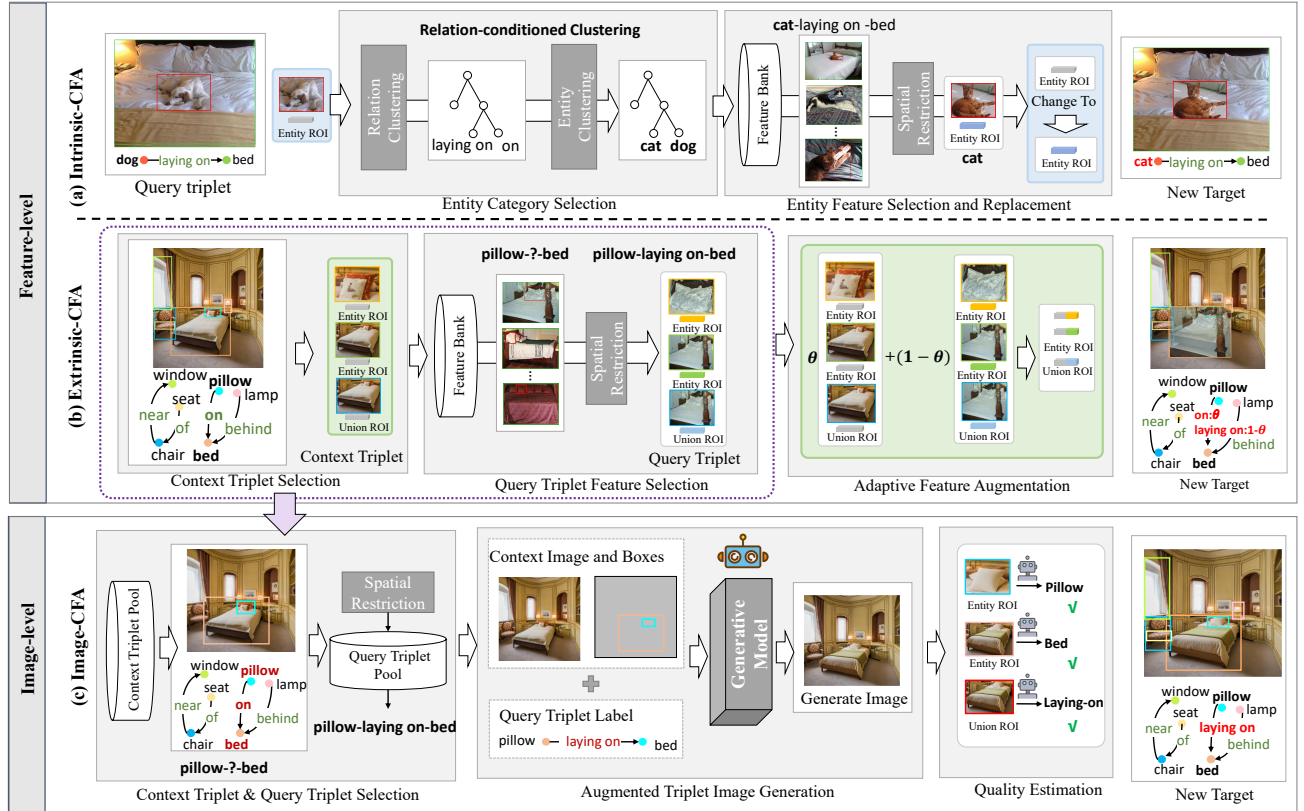


Fig. 5: The pipeline of feature-level and image-level augmentation strategy. Feature-level strategy consists of two approaches to generate new compositions of triplet features tailored for intrinsic and extrinsic diversity enhancement respectively, *i.e.*, (a) Intrinsic-CFA and (b) Extrinsic-CFA. While image-level strategy generates new visual appearance of relation triplet by generative models to ensure the augmentation quality, *i.e.*(c) Image-CFA.

and proposal b_i , they use an object context encoder Enc_{obj} to extract the contextual entity representation f_i :

$$f_i = \text{Enc}_{obj}(v_i \oplus b_i), \quad (2)$$

where \oplus denotes concatenation. Then, they use an object classifier Cls_{obj} to predict their entity categories:

$$\hat{o}_i = \text{Cls}_{obj}(f_i). \quad (3)$$

Predicate Classification $P(\mathcal{R}|\mathcal{O}, \mathcal{B}, I)$. This step predicts the predicate categories of every two proposals in \mathcal{B} along with their entity categories. First, they use a relation context encoder Enc_{rel} to extract the refined entity feature \tilde{f}_i :

$$\tilde{f}_i = \text{Enc}_{rel}(v_i \oplus f_i \oplus w_i), \quad (4)$$

where w_i is the GloVe embedding [32] of predicted \hat{o}_i . It is worth noting that both Enc_{cls} and Enc_{rel} often adopt a sequence model (*e.g.*, Bi-LSTM [43], Tree-LSTM [35], or Transformer [42]) to better capture context. After relation feature encoding, they use a relation classifier Cls_{rel} to predict the relation \hat{r}_{ij} between any two subject-object pairs:

$$\hat{r}_{ij} = \text{Cls}_{rel}([\tilde{f}_i \oplus \tilde{f}_j] \circ u_{ij}), \quad (5)$$

where \circ denotes element-wise product, and u_{ij} denotes the visual feature of the union box b_{ij} .

3.2 Feature-level CFA

In this paper, we treat a relation triplet feature² in SGG as a combination of two components: intrinsic feature and extrinsic feature, which refer to the intrinsic information (*i.e.*, the subject and object itself) and extrinsic information (*i.e.*, the contextual objects and stuff), respectively. Correspondingly, our feature-level CFA consists of intrinsic-CFA and extrinsic-CFA to augment these two types of features. For ease of presentation, we call the “targeted tail predicate triplet whose feature to be enhanced” as “**query triplet**”, and the “relation triplet whose image is used to provide context” as “**context triplet**”. Besides, to facilitate the feature augmentation, we store all the visual features of all tail predicate triplets (*i.e.*, visual features v of two entities and their union feature u) in a **feature bank** before training. Besides, we adopt the repeat factor $\eta = \max(1, \eta_r)$ [12, 23] to sample images to provide enough context triplet and query triplet

for augmentation, where $\eta_r = \sqrt{\lambda/f_r}$, f_r is the frequency of predicate category r on the entire dataset, and λ is hyperparameter. The unbiased SGG pipeline with feature-level CFA is shown in Fig. 4.

3.2.1 Intrinsic-CFA

Intrinsic-CFA enhances the feature of query triplet by replacing its visual features of entities (*i.e.*, subject and object). It consists of two steps: *entity category selection* and *entity feature selection and replacement* (*cf.* Fig. 5(a)). During training, we randomly select a query triplet from a batch of images, and randomly select one of its entity features as input. Then we put it into the Intrinsic-CFA module (*cf.* Fig. 4). Next, we detailedly introduce each step.

Entity Category Selection. This step is used for determining the category to which the entity feature of the query triplet is replaced. Firstly, we propose a novel **relation-conditioned entity clustering** that organizes entity categories based on their semantic role in a triplet. The framework consists of the following procedures.

(1) Predicate Clustering. To maintain consistency in entity substitutions, we first group predicates into several clusters. The clustering process utilizes three similarity measures:

- **Pattern Similarity:** This metric quantifies the degree of functional overlap between predicates by analyzing the frequency with which they govern similar subject-object pairs. Formally, for two predicate categories c_{p_i} and c_{p_j} , pattern similarity is defined as:

$$Sim_p(c_{p_i}, c_{p_j}) = \frac{|L_{so}|}{d(c_{p_i}) + d(c_{p_j}) - |L_{so}|}, \quad (6)$$

where $|L_{so}|$ denotes the number of common subject-object associations and $d(c_{p_i})$ denotes the sample number with the predicate category c_{p_i} in the dataset.

- **Context Similarity:** This measure evaluates the extent to which two predicates appear in similar environmental contexts by comparing their co-occurring entities:

$$Sim_c(c_{p_i}, c_{p_j}) = \frac{|L_e|}{d_{co}(c_{p_i}) + d_{co}(c_{p_j}) - |L_e|}, \quad (7)$$

where $|L_e|$ denotes the number of entity categories that co-occur with both c_{p_i} and c_{p_j} in the same image. The term $d_{co}(c_{p_i})$ represents the number of images in which predicate category c_{p_i} appears.

- **Semantic Similarity:** To capture semantic alignment, we compute the Euclidean distance between two predicate categories in a pre-trained embedding space:

$$Sim_s(c_{p_i}, c_{p_j}) = \|\mathbf{e}_{p_i} - \mathbf{e}_{p_j}\|_2. \quad (8)$$

The final similarity score for predicate clustering is a weighted sum of these three measures.

(2) Predicate Category Merging. Once predicate clusters are established, associated subject and object categories within each cluster are merged to ensure consistency. Overlapping subject categories among clustered predicates are unified, guaranteeing consistent treatment of interchangeable subjects across relational structures. Likewise, object categories governed by these clustered predicates are merged, preserving the relational and contextual properties of entity substitutions.

For instance, if the predicates standing on and sitting on belong to the same cluster, their subject categories (*e.g.*, dog, cat, person) and object categories (*e.g.*, chair, floor, bed) are merged accordingly.

(3) Entity Category Clustering. After merging, we further cluster entity categories within the same predicate clusters to identify interchangeable entities. The clustering process follows a methodology similar to predicate clustering and employs three similarity measures. Fig. 6 shows an example of pattern and context similarity between cat and dog:

- **Pattern Similarity:** This metric evaluates the extent to which two entity categories participate in similar relational structures. It is computed as:

$$Sim_p(c_{e_i}, c_{e_j}) = \frac{|L_{sp}|}{d_{out}(c_{e_i}) + d_{out}(c_{e_j}) - |L_{sp}|} + \frac{|L_{po}|}{d_{in}(c_{e_i}) + d_{in}(c_{e_j}) - |L_{po}|}, \quad (9)$$

where $|L_{sp}|$ and $|L_{po}|$ represent the number of common subject-predicate and predicate-object associations. Terms $d_{in}(c_{e_i})$ and $d_{out}(c_{e_i})$ denote the number of incoming and outgoing edges of entity category c_{e_i} .

- **Context Similarity:** Similarly, this similarity measures the context’s overlap of two entity categories in images:

$$Sim_c(c_{e_i}, c_{e_j}) = \frac{|L_e|}{d_{co}(c_{e_i}) + d_{co}(c_{e_j}) - |L_e|}. \quad (10)$$

- **Semantic Similarity:** As with predicates, it’s the distance between two entity semantic embeddings:

$$Sim_s(c_{e_i}, c_{e_j}) = \|\mathbf{e}_{e_i} - \mathbf{e}_{e_j}\|_2. \quad (11)$$

Entire clustering algorithm and results are in the **appendix**.

Entity Feature Selection and Replacement. This step selects an entity feature from the feature bank based on the selected entity category and replaces it with the query triplet. Specifically, we first update a new entity category of query triplet (*e.g.*, cat-laying on-bed). Then, we select all triplet features with the same category as query triplet from feature bank as candidates (*cf.* Fig. 5(a)). And we utilize spatial restriction to filter unreasonable triplet features.

Spatial Restriction. In real augmentation, even if the two entity categories appear to be interchangeable, the positions of the subject and object after replacement may not make sense. For example, in VG dataset (*cf.* **appendix**), though

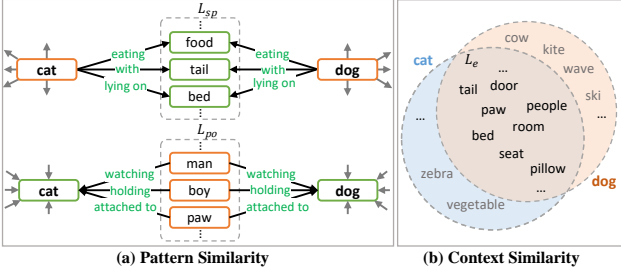


Fig. 6: Illustration of the pattern and context similarity between entity categories `cat` and `dog`. a) White boxes are the behavior patterns common to two categories. b) Blue and red circles are entity categories that co-occur with `cat` and `dog`, respectively.

category `hat` and `shoe` are in the same cluster, directly replacing `hat` with `shoe` would place the `shoe` on the head and make it contrary to common sense.

To further ensure the rationality of the replacement of the two entity features, we use the cosine similarity of the relative spatial position of subject-object of the query triplet and the selected triplet from the feature bank as restriction:

$$Sim_d(\mathbf{p}_i, \mathbf{p}_j) = \frac{\mathbf{p}_i \cdot \mathbf{p}_j}{|\mathbf{p}_i||\mathbf{p}_j|}, \quad (12)$$

where \mathbf{p}_i is the spatial vector from the center of the subject bbox to the center of object bbox. When the Sim_d between \mathbf{p}_i of the query triplet and \mathbf{p}_j of the selected triplet from the feature bank is larger than the threshold σ , the entity feature of the selected triplet is reasonable for replacement.

During replacement, we randomly select one of the reasonable entity features and replace it into query triplet and change the original entity target to the new entity category.

Highlights. In the original intrinsic-CFA of CFA [21], we clustered entities uniformly, ignoring predicate-driven semantic discrepancy (e.g., `kite` and `umbrella` are replaceable for `holding`, but an `umbrella` is ill-suited for `flying` in the sky where a `kite` fits). In this paper, we devise a relation-conditioned entity clustering, allowing more accurate, predicate-aware entity groupings. This approach, for instance, discerns the similarity of `kite` and `umbrella` for `holding` versus their distinct roles for `flying` in, yielding more precise entity selection.

3.2.2 Extrinsic-CFA

Extrinsic-CFA aims to enrich the feature of the query triplet through the extrinsic information (i.e., the context formed by all the entities of an image) of context triplets. Different from the intrinsic-CFA, we select context triplet during training for computation efficiency. Extrinsic-CFA includes three steps: *context triplet selection*, *query triplet feature selection*, and *adaptive feature augmentation* (cf., Fig. 5(b)). Then, we detail each step of extrinsic-CFA.

Context Triplet Selection. For each image, this step selects context triplets for extrinsic-CFA. Specifically, we randomly select context triplets with foreground or background predicate categories to provide more extrinsic information. *For foreground context triplets*, considering the large variation in the number of triplet samples for different predicate categories, we randomly sample the context triplets by using probability $p = (\eta - \eta_r)/\eta \times \gamma$ during training, where γ is hyperparameter. *For background context triplets*, we randomly select them with the same subject-object pair as the tail predicate triplet in the whole dataset.

Query Triplet Feature Selection. This step selects a query triplet with its features for the feature augmentation. Specifically, we select triplets with the same subject-object categories (e.g., `pillow-bed`) as the context triplet (e.g., `pillow-on-bed`) from feature bank as the candidate query triplets. Then, we implement the same spatial restriction as intrinsic-CFA to filter unreasonable triplets. Finally, we randomly select one of the reasonable triplets as the query triplet (e.g., `pillow-laying on-bed`), and its features are utilized for augmentation (cf. Fig. 5(b)).

Adaptive Feature Augmentation. To enhance the extrinsic features of tail predicate triplets while concurrently mitigating the impact on other triplets of the original image, we devise a novel adaptive mixup operation. This operation blends a selected query triplet (e.g., `pillow-laying on-bed`) with a context triplet (e.g., `pillow-on-bed`), as depicted in Fig. 5(b). The adaptive mixup is formulated as follows:

$$\begin{aligned} \theta &= 1 - \alpha \frac{\mathbf{e}_p \cdot \mathbf{e}'_p}{|\mathbf{e}_p||\mathbf{e}'_p|}, \\ \tilde{\mathbf{v}}_s &= \theta \mathbf{v}_s + (1 - \theta) \mathbf{v}'_s, \\ \tilde{\mathbf{v}}_o &= \theta \mathbf{v}_o + (1 - \theta) \mathbf{v}'_o, \\ \tilde{\mathbf{u}} &= \theta \mathbf{u} + (1 - \theta) \mathbf{u}', \end{aligned} \quad (13)$$

where \mathbf{e}_p and \mathbf{e}'_p denote the semantic embedding of relation category in context triplet (e.g., `on`) and selected query triplet (e.g., `laying on`), respectively. The parameters α is used to control the value range of θ . \mathbf{v}'_s (\mathbf{v}_s) and \mathbf{v}'_o (\mathbf{v}_o) denote the visual features of the subject and object of the query triplet (context triplet), respectively. The \mathbf{u}' (\mathbf{u}) denotes the visual feature of the union box of the query triplet (context triplet). Similarly, the predicate target ground-truth r of the context triplet is mixed:

$$\tilde{r} = \theta r + (1 - \theta) r', \quad (14)$$

where θ is utilized to control the degree of mixup operation.

After the mixup operation, the query triplet feature can be enhanced in context modeling (cf. Fig. 4) by leveraging the extrinsic features of the context triplet.

Highlights. In CFA [21], we employed a fixed θ for feature augmentation. It fails to adapt to varying semantic similarities between query and context triplets, risking under-enhancement of tail predicate triplets or feature corruption

via suboptimal contextual blending. In this paper, we propose an adaptive feature augmentation strategy, enabling the mixup coefficient θ to dynamically adjust based on predicate similarity between query and context triplets. This facilitates targeted enrichment of tail predicates using relevant contexts while preventing feature distortion from less aligned ones, ultimately boosting model robustness.

3.3 Image-level CFA

Although the above mentioned methods effectively augment the diversity of both extrinsic and intrinsic features of predicates, the constructed feature space is still limited in the dataset domain. In order to maximally infer the real feature space of predicates and learn the true data distribution, we also propose an image-level augmentation method that leverages large generative models [26] to create new visual appearance of relation triplets. Image-level CFA includes three steps: *context triplet and query triplet selection*, *augmented triplet image generation*, and *quality estimation* (cf., Fig. 5(c)). Then, we detail each step of Image-level CFA.

Context Triplet and Query Triplet Selection. For each image, this step selects context triplets and query triplet to be augmented for image-level augmentation. We select context triplets with foreground predicate categories to provide extrinsic information. We apply the same sampling strategy as the way of extrinsic-CFA in Sec. 3.2.2, *i.e.*, we randomly sample the context triplets by using probability $p = (\eta - \eta_r)/\eta \times \gamma$ during training, where γ is hyperparameter. We also apply the same strategy as the way of extrinsic-CFA in Sec. 3.2.2 to select query triplet, but we only use its categories and grounding information of entities and predicate. Then we send them with context triplets together to generate new visual images.

Augmented Triplet Image Generation. This step is to generate new image with context and query triplets. The main challenge is to ensure the rationality of generated image with query triplet. Taking the power of recent generative models, *e.g.*, GLIGEN [26], we generate new samples conditioned on more input information apart from text to control the generation process, *e.g.*, bounding boxes and reference images.

Specifically, for each image I , suppose that the subject and object of the selected query triplet is i and j , and the corresponding bounding boxes are $\mathbf{b}_i, \mathbf{b}_j \in \mathcal{B}$ respectively. Our aim is to generate images with new visual appearance of entity i and j conditioned on the context information. We send the instruction \mathbf{g} to the grounded text-to-image model GLIGEN [26], which is a composition of reference image and query triplet information:

$$\mathbf{g} = (\mathbf{e}_i, \mathbf{e}_j, r_{ij}, I), \text{ with } \mathbf{e}_i = (\mathbf{b}_j, o_i \in \mathcal{O}) \quad (15)$$

where \mathbf{e}_i are the information of entity i with its category and bounding box, and $r_{ij} \in \mathcal{R}$ is the triplet predicate category.

After pretrained with multiple input modalities besides text input, GLIGEN [26] is able to generate improved quality image with grounding conditions. Some generated samples are displayed in Fig. 8.

Quality Estimation. After generating the new visual appearance of entities, we have to check their quality and make sure their category are remained consistent. We send the cropped regions of generated entities and triplets into the pretrained CLIP model [33] to predict the classification scores. Only the correctly classified samples will be selected as the augmented datas to participate in the training process of SGG models.

3.4 Training Objectives

Cross-Entropy Losses. The optimization objective of commonly used SGG models mainly includes the cross-entropy of entity and relation classification, the loss functions are:

$$L_{obj} = \sum_i \text{XE}(\hat{o}_i, o_i), \quad L_{rel} = \sum_{ij} \text{XE}(\hat{r}_{ij}, r_{ij}), \quad (16)$$

where \hat{o}_i is the predicted entity category and o_i is the ground-truth entity category. \hat{r}_{ij} is the predicted predicate category and r_{ij} is the ground-truth predicate category.

Contrastive Loss. Due to the pattern changes between the entity features after mixup and original entity features, using only XE losses may result in performance drops in entity classification. To maintain the discriminative entity features after mixup, we further apply a contrastive loss [4]:

$$L_{cl} = -\log \frac{\exp(Sim_e(\mathbf{z}_i, \mathbf{z}_j)/\tau)}{\sum_{k=1}^{2M} 1_{[k \neq i]} \exp(Sim_e(\mathbf{z}_i, \mathbf{z}_k)/\tau)}, \quad (17)$$

where \mathbf{z}_i and \mathbf{z}_j represent the output of the layer before predictor of original entity and the entity after mixup operation, M is the number of entities in which the mixup operation is performed. $Sim_e(\cdot, \cdot)$ is the cosine similarity.

Training. During training, the total loss includes the cross-entropy losses L_{obj} , L_{rel} and the extra contrastive loss L_{cl} :

$$L_{total} = L_{rel} + L_{obj} + \beta L_{cl}, \quad (18)$$

where β is used to regulate the magnitude of loss.

4 Experiments

4.1 Experimental Settings and Details

Tasks. We evaluated models in three tasks [40]: 1) *Predicate Classification (PredCls)*: Predicting the predicate category given all ground-truth entity bboxes and categories. 2) *Scene Graph Classification (SGCls)*: Predicting categories of the predicate and entity given all ground-truth entity bboxes.

SGG Models	PredCls						SGCls						SGGen							
	mR@K			R@K			mR@K			R@K			mR@K			R@K			Mean	
	50	100		50	100	Mean		50	100		50	100	Mean		50	100		50	100	Mean
Motifs [43] _{CVPR'18}	16.5	17.8	65.5	67.2	41.8	8.7	9.3	39.0	39.7	24.2	5.5	6.8	32.1	36.9	20.3					
VCTree [35] _{CVPR'19}	17.1	18.4	65.9	67.5	42.2	10.8	11.5	45.6	46.5	28.6	7.2	8.4	32.0	36.2	20.9					
Transformer [37] _{NIPS'17}	17.9	19.6	63.6	65.7	41.7	9.9	10.5	38.1	39.2	24.4	7.4	8.8	30.0	34.3	20.1					
BGNN [23] _{CVPR'21}	30.4	32.9	59.2	61.3	45.9	14.3	16.5	37.4	38.5	26.7	10.7	12.6	31.0	35.8	22.5					
Motifs+PCPL [41] _{ACMMM'20}	24.3	26.1	54.7	56.5	40.4	12.0	12.7	35.3	36.1	24.0	10.7	12.6	27.8	31.7	20.7					
Motifs+DLFE [5] _{ACMMM'21}	26.9	28.8	52.5	54.2	40.6	15.2	15.9	32.3	33.1	24.1	11.7	13.8	25.4	29.4	20.1					
Motifs+BPL-SA [11] _{ICCV'21}	29.7	31.7	50.7	52.5	41.2	16.5	17.5	30.1	31.0	23.8	13.5	15.6	23.0	26.9	19.8					
Motifs+NICE [19] _{CVPR'22}	29.9	32.3	55.1	57.2	43.6	16.6	17.9	33.1	34.0	25.4	12.2	14.4	27.8	31.8	21.6					
Motifs+IETrans [44] _{ECCV'22}	30.9	33.6	54.7	56.7	44.0	16.8	17.9	32.5	33.4	25.2	12.4	14.9	26.4	30.6	21.1					
Motifs+CFA [21] _{ICCV'23}	35.7	38.2	54.1	56.6	46.2	17.0	18.4	34.9	36.1	26.6	13.2	15.5	27.4	31.8	22.0					
Motifs+DPL [16] _{ECCV'24}	33.7	37.4	54.4	56.3	45.5	18.5	20.1	32.6	33.8	26.3	13.0	15.6	24.5	28.7	20.5					
Motifs+MCFA (ours)	35.8	38.3	54.3	56.8	46.3	17.9	19.4	35.5	36.7	27.4	14.0	16.3	27.1	31.6	22.3					
VCTree+PCPL [41] _{ACMMM'20}	22.8	24.5	56.9	58.7	40.7	15.2	16.1	40.6	41.7	28.4	10.8	12.6	26.6	30.3	20.1					
VCTree+DLFE [5] _{ACMMM'21}	25.3	27.1	51.8	53.5	39.4	18.9	20.0	33.5	34.6	26.8	11.8	13.8	22.7	26.3	18.7					
VCTree+BPL-SA [11] _{ICCV'21}	30.6	32.6	50.0	51.8	41.3	20.1	21.2	34.0	35.0	27.6	13.5	15.7	21.7	25.5	19.1					
VCTree+NICE [19] _{CVPR'22}	30.7	33.0	55.0	56.9	43.9	19.9	21.3	37.8	39.0	29.5	11.9	14.1	27.0	30.8	21.0					
VCTree+IETrans [44] _{ECCV'22}	30.3	33.9	53.0	55.0	43.1	16.5	18.1	32.9	33.8	25.3	11.5	14.0	25.4	29.3	20.1					
VCTree+CFA [21] _{ICCV'23}	34.5	37.2	54.7	57.5	46.0	19.1	20.8	42.4	43.5	31.5	13.1	15.5	27.1	31.2	21.7					
VCTree+DPL [16] _{ECCV'24}	35.3	37.9	54.0	55.8	45.8	19.2	21.3	32.6	33.9	26.8	13.2	15.9	27.0	31.4	21.9					
VCTree+MCFA (ours)	35.4	38.2	54.0	56.9	46.1	21.0	23.3	41.8	42.9	32.3	13.4	15.8	27.2	31.6	22.0					
Transformer+IETrans [44] _{ECCV'22}	30.8	34.5	51.8	53.8	42.7	17.4	19.1	32.6	33.5	25.7	12.5	15.0	25.5	29.6	20.7					
Transformer+CFA [21] _{ICCV'23}	30.1	33.7	59.2	61.5	46.1	15.7	17.2	36.3	37.3	26.6	12.3	14.6	27.7	32.1	21.7					
Transformer+MCFA (ours)	32.4	34.4	58.9	61.0	46.7	16.4	17.6	36.7	37.9	27.2	12.6	15.1	27.4	32.0	21.8					

Table 1: Performance (%) of the SOTA trade-off SGG models on VG [18]. “Mean” is the average of mR@50/100 and R@50/100.

SGG Models	PredCls			SGCls			SGGen		
	mR@20	mR@50	mR@100	mR@20	mR@50	mR@100	mR@20	mR@50	mR@100
Motifs+TDE [36] _{CVPR'20}	18.5	25.5	29.1	9.8	13.1	14.9	5.8	8.2	9.8
Motifs+CogTree [42] _{IJCAI'21}	20.9	26.4	29.0	12.1	14.9	16.1	7.9	10.4	11.8
Motifs+RTPB [1] _{AAAI'22}	28.8	35.3	37.7	16.3	20.0	21.0	9.7	13.1	15.5
Motifs+PPDL [24] _{CVPR'22}	27.9	32.2	33.3	15.8	17.5	18.2	9.2	11.4	13.5
Motifs+GCL [10] _{CVPR'22}	30.5	36.1	38.2	18.0	20.8	21.8	12.9	16.8	19.3
Motif+HML [7] _{ECCV'22}	30.1	36.3	38.7	17.1	20.8	22.1	10.8	14.6	17.3
Motifs+CFA [‡] [21] _{ICCV'23}	31.5	39.9	43.0	17.3	20.9	22.4	11.2	15.3	18.1
Motifs+MCFA[‡] (ours)	31.8	40.3	43.5	17.7	21.3	22.7	11.9	15.8	18.6
VCTree+TDE [36] _{CVPR'20}	18.4	25.4	28.7	8.9	12.2	14.0	6.9	9.3	11.1
VCTree+CogTree [42] _{IJCAI'21}	22.0	27.6	29.7	15.4	18.8	19.9	7.8	10.4	12.1
VCTree+RTPB [1] _{AAAI'22}	27.3	33.4	35.6	20.6	24.5	25.8	9.6	12.8	15.1
VCTree+PPDL [24] _{CVPR'22}	29.7	33.3	33.8	20.3	21.8	22.4	9.1	11.3	13.3
VCTree+GCL [10] _{CVPR'22}	31.4	37.1	39.1	19.5	22.5	23.5	11.9	15.2	17.5
VCTree+HML [7] _{ECCV'22}	31.0	36.9	39.2	20.5	25.0	26.8	10.1	13.7	16.3
VCTree+CFA [‡] [21] _{ICCV'23}	31.6	39.2	42.5	21.5	26.3	28.3	10.8	15.1	17.9
VCTree+MCFA[‡] (ours)	32.3	40.2	43.2	21.7	27.2	29.2	11.0	15.3	18.0
Transformer+CogTree [42] _{IJCAI'21}	22.9	28.4	31.0	13.0	15.7	16.7	7.9	11.1	12.7
Transformer+HML [7] _{ECCV'22}	27.4	33.3	35.9	15.7	19.1	20.4	11.4	15.0	17.7
Transformer+CFA [‡] [21] _{ICCV'23}	31.2	38.6	41.5	17.2	20.9	22.7	10.6	15.0	17.9
Transformer+MCFA[‡] (ours)	31.4	38.9	42.2	17.5	21.5	23.1	10.8	15.1	18.1

Table 2: Performance (%) of the SOTA tail-focused SGG models on VG [18]. [‡] means using the component prior knowledge.

3) **Scene Graph Generation (SGGen):** Detecting all entities and their pairwise predicates.

Metrics. We evaluated SGG models on three metrics: 1) *Recall@K (R@K)*: It indicates the proportion of ground-truths that appear among the top-*K* confident predicted relation triplets. 2) *mean Recall@K (mR@K)*: It is the average of R@K scores which are calculated for each predicate category separately. 3) **Mean**: It is the average of all R@K and mR@K scores. Since R@K favors head predicates while

mR@K favors tail predicates, the Mean can better reflect the overall performance of all predicates [19].

Datasets. We conducted all experiments on two datasets: **VG** and **GQA**. 1) **VG**: We followed the widely-used strategy [40] to split dataset (*i.e.*, 75K/32K images for train/test, 150 object categories and 50 predicate categories). Besides, 5K images within the training set are sampled as val set following [36]. All predicate categories are divided into three groups {head, body, tail} based on the number of samples

Models	PredCls	SGCls	SGGen
	mR@50/100	mR@50/100	mR@50/100
Motifs [43]	13.9 / 14.7	7.2 / 7.5	5.5 / 6.6
+CFA	31.7 / 33.8	14.2 / 15.2	11.6 / 13.2
+DPL [16]	31.6 / 33.9	13.3 / 14.4	11.1 / 13.1
+MCFA	32.5 / 33.9	14.7 / 15.8	12.0 / 13.8
VCTree [35]	14.4 / 15.3	6.1 / 6.6	5.8 / 6.0
+CFA	33.4 / 35.1	14.1 / 15.0	10.8 / 12.6
+DPL [16]	31.4 / 34.3	13.3 / 14.9	11.9 / 13.7
+MCFA	33.8 / 35.5	14.3 / 15.4	11.1 / 13.1
Transformer [37]	15.2 / 16.1	7.5 / 7.9	6.9 / 7.8
+CFA	27.8 / 29.4	16.2 / 16.9	13.4 / 15.3
+MCFA	28.6 / 30.4	16.6 / 17.2	13.5 / 15.6

Table 3: Performance (%) of the SGG models on GQA [15].

as [28]. 2) **GQA**: We followed the prior work [10] to split dataset (*i.e.*, 70%/30% of the images for train/test, 200 object categories and 100 predicate categories). Similarly, 5K images within the training set are sampled as val set. We utilized the same group category ratio as VG to divide all predicate categories into {head, body, tail} groups.

Implementation Details. Following the training protocol in prior SGG works [36], we adopted the object detector Faster R-CNN with the ResNeXt-101-FPN [27] backbone trained by [36] to detect all the bounding boxes and extract their visual features. The parameters of the backbone were kept frozen during the training. This detector could achieve 28.14 mAP on the VG test set (*i.e.*, using 0.5 IoU threshold for evaluation). **To avoid messy hyperparameter tuning, most of the hyperparameters follow previous works.** More specifically, the hyperparameters λ and γ were set to 0.07 and 0.7 in MCFA (*cf.*, Sec. 3.2). The weights of pattern, context and semantic similarity were 1.0, 1.0 and 0.01 in intrinsic-CFA (*cf.*, Sec. 3.2.1). The hyperparameter α used to control the value range of adaptive mixup coefficient θ was set to 0.5 in extrinsic-CFA (*cf.*, Sec. 3.2.2). The threshold σ was set to 0.5 in spatial restriction (*cf.*, Sec. 3.2.2). The β was set to 0.1 to regulate the loss during training (*cf.*, Sec. 3.4). In this paper, SGD optimizer was used to train the model. The batch size was set to 12 and the initial learning rate was set to 0.01. After the performance on the val set reached the plateau period, the learning rate would be decayed by 10 for two times. All experiments were carried out with PyTorch and NVIDIA 2080Ti GPU.

4.2 Comparison with State-of-the-Arts

Setting. Due to the model-agnostic nature, we equipped our MCFA with three strong two-stage SGG baselines: Motifs [43], VCTree [35] and Transformer [37], and they are denoted as **Motifs+MCFA**, **VCTree+MCFA**, and **Transformer+MCFA**, respectively. In addition, due to the limited diversity of tail predicate components [25], it has a high correlation with the category of subject & object.

Thus, we further equip our three models with the component prior knowledge collected from the dataset to further improve the performance of the tail predicates. And they are denoted as **Motifs+MCFA[‡]**, **VCTree+MCFA[‡]**, and **Transformer+MCFA[‡]** (More details about the priors are discussed in appendix).

Baselines. We compared our methods with the state-of-the-art (SOTA) models in the VG dataset (Table 1 and Table 2) and the GQA dataset (Table 3). Specifically, these models can be divided into three groups: 1) **Model-specific designs**: Motifs, VCTree, Transformer, and BGNN [23]. 2) **Model-agnostic trade-off** methods: consider the performance of all predicates comprehensively (*i.e.*, higher Mean), *e.g.*, PCPL [41], DLFE [5], BP-LSA [11], NICE [19], IETrans [44], CFA [21], and DPL [16]. 3) **Model-agnostic tail-focused** methods: improve tail predicates performance at the expense of excessively sacrificing the head (*i.e.*, higher mR@K and R@50 less than 50.0% on PredCls), *e.g.*, TDE [36], CogTree [42], RTPB [1], PPDL [24], GCL [10], and HML [7]. For a fair comparison, we compared with the methods in the last two groups.

Quantitative Results on VG. Analysis of the **trade-off** methods presented in Table 1 highlights two key observations: 1) Compared to three strong baselines (*i.e.*, Motifs, VCTree, and Transformer), MCFA significantly enhances performance on the mR@K metric across all three experimental settings. 2) MCFA strikes the most effective trade-off between R@K and mR@K, evidenced by the highest Mean score. Notably, it surpasses the previous SOTA trade-off method, CFA [21], which itself adeptly minimized performance decline on head predicates (R@K) while preserving tail performance (mR@K), in this crucial Mean metric under all settings. Turning to the **tail-focused** methods detailed in Table 2, MCFA[‡], which incorporates further strategies dedicated to improving tail predicate performance, achieves the highest mR@K values. It outperforms prominent SOTA tail-focused approaches, *i.e.*, HML [7] and CFA [21], on the mR@K metric across all evaluated settings. Additional experimental analyses are provided in the appendix.

Quantitative Results on GQA. As demonstrated in Table 3, MCFA also markedly enhances mR@K performance over three strong baselines (*i.e.*, Motif, VCTree, and Transformer) on the large-scale GQA dataset. These results certify the generalizability and effectiveness of our method.

4.3 Ablation Studies

Feature-Level Augmentation. We assessed the impact of each component within our feature-level CFA using the Motifs [43] baseline under the SGGen setting. Feature-level CFA comprises three primary components: replacing intrinsic features (**IN**), mixing extrinsic features of foreground

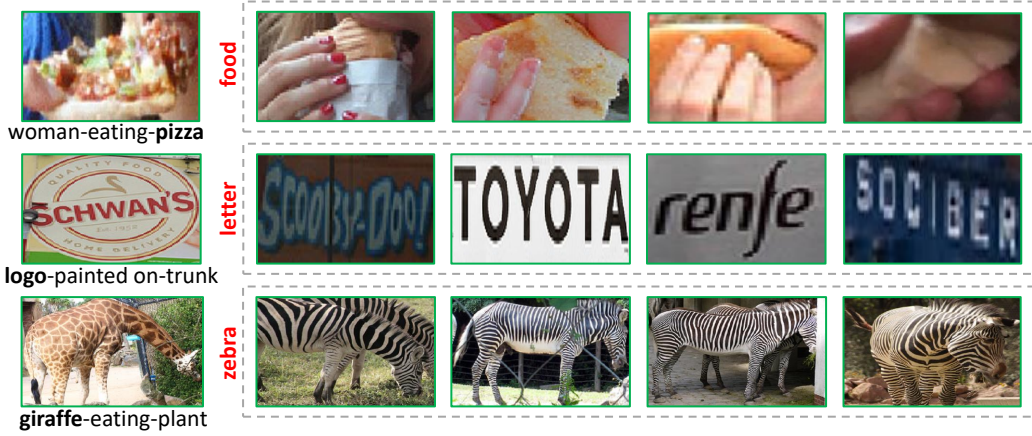


Fig. 7: The examples of reasonable entities for the query triplet in intrinsic-CFA. The lefts are original entities of the query triplets. The rights are some alternate entity categories (red) and their samples (gray boxes) for each query triplet to replace.

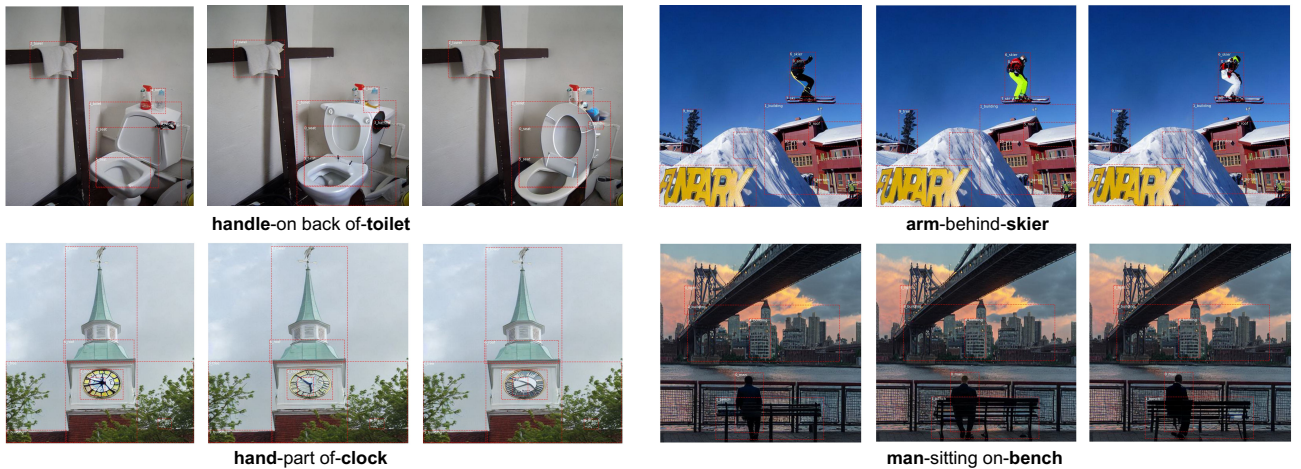


Fig. 8: The examples of generated triplets for image-level augmentation.

Component			SGCls		
IN	EX-fg	EX-bg	mR@50 / 100	R@50 / 100	Mean
			8.7 / 9.3	39.0 / 39.7	24.2
✓			11.6 / 12.4	37.4 / 38.6	25.0
	✓		15.6 / 16.5	34.9 / 36.2	25.8
		✓	14.3 / 15.7	35.9 / 37.0	25.7
✓	✓		17.0 / 18.0	35.8 / 36.9	26.9
✓		✓	17.1 / 18.3	35.4 / 37.0	27.0
	✓	✓	17.8 / 18.8	34.4 / 35.6	26.7
✓	✓	✓	17.9 / 19.4	35.5 / 36.7	27.4

Table 4: Ablation study on each component in feature-level augmentation [18]. Motifs [43] is used in all ablations on VG [18]. IN: Replace the intrinsic features. Ex-fg: Mix up the extrinsic features of foreground triplets. Ex-bg: Mix up the extrinsic features of background triplets.

triplets (**EX-fg**), and mixing extrinsic features of background triplets (**EX-bg**). The results, reported in Table 8, lead to the following observations: 1) Employing only the

Similarity			SGCls		
Pattern	Context	Semantic	mR@50 / 100	R@50 / 100	Mean
✓			16.1 / 17.3	34.4 / 35.8	25.9
	✓		17.1 / 18.3	36.1 / 37.3	27.2
		✓	18.1 / 19.1	33.5 / 34.8	26.4
✓	✓		16.9 / 18.2	35.0 / 36.3	26.6
✓		✓	17.4 / 18.5	35.7 / 36.8	27.1
✓	✓	✓	16.5 / 17.6	37.0 / 38.2	27.3
✓	✓	✓	17.9 / 19.4	35.5 / 36.7	27.4

Table 5: Ablation study on each similarity in clustering of intrinsic-MCFA.

IN component yields a marginal improvement in mR@K (e.g., 2.9%–3.1% gains) while slightly degrading R@K performance (a 1.1%–1.6% loss). This is likely attributable to the limited diversity among tail predicate triplets, meaning that feature variety remains constrained even after intrinsic feature replacement. 2) Both EX-fg and EX-bg components substantially enhance mR@K and also achieve R@K scores

K_p	SGCIs		
	mR@50 / 100	R@50 / 100	Mean
10	17.5 / 18.9	35.3 / 37.1	27.2
20	17.9 / 19.4	35.5 / 36.7	27.4
50	17.3 / 18.4	35.5 / 37.3	27.1

Table 6: Ablation study on the number of predicate clusters K_p of intrinsic-CFA.

relative to the baseline. For instance, mR@100 increases to 18.0% from the baseline’s 9.3%, and R@100 maintains 18.8% with these components. 3) Combining all three components (IN, EX-fg, and EX-bg) achieves the optimal trade-off, *i.e.*, the highest Mean score.

Similarity of Clustering in Intrinsic-CFA. We investigated the impact of three distinct similarity measures (pattern, context, and semantic) on clustering within intrinsic-CFA, utilizing the Motifs [43] model as a baseline under the SGCIs setting. Results presented in Table 5 demonstrate that relying solely on pattern similarity yields the poorest SGG performance. This deficiency occurs since pattern-based similarity alone disregards crucial contextual and semantic information, which is essential for guiding meaningful cluster formation. For instance, while both a `boat` and a `car` may share a “ridable” pattern, substituting a `car` for a `boat` would be semantically invalid in a maritime context (*e.g.*, on the sea), as a `car` cannot operate there. Conversely, when contextual and semantic similarities are integrated into the analysis, SGG performance becomes substantially more robust, culminating in the highest Mean.

Different Cluster Number. We performed $K_p \in \{10, 20, 50\}$ to evaluate the impact of the number of predicate clusters under SGCIs setting with Motifs [43]. As illustrated in [21], since when entity cluster number K_e set to 15, there is a larger selection range of replaceable entity categories and richer feature diversity of tail predicate triplets, we use same entity cluster number setting. All results are reported in Table 6. We find that $K_p = 20$ works best in mR@K. The reason may be that when K_p is smaller, such as 10, the predicate clusters might be too coarse, grouping semantically distinct predicates together. This over-generalization can lead to less precise entity selection by potentially merging entities that play truly different roles across these distinct predicates, thereby reducing the discriminativeness for specific relations. When K_p is larger (*e.g.*, 50), the predicate clusters may become overly granular, which could prevent the model from capturing broader semantic similarities between closely related predicates. Consequently, this limits the effectiveness of relation-conditioned entity merging as each predicate cluster becomes too specific and offers fewer possibilities for generalization.

Mixup Parameter θ in Extrinsic-CFA. As mentioned in Sec. 3.2.2, θ indicates the proportion of selected features in final augmented features. We investigated $\theta \in \{0.0, 0.5, 1.0\}$

θ	SGCIs		
	mR@50 / 100	R@50 / 100	Mean
0.0	16.9 / 17.9	35.2 / 36.5	26.6
0.5	17.1 / 18.6	36.0 / 37.2	27.2
1.0	11.6 / 12.4	37.4 / 38.6	25.0
Adap	17.9 / 19.4	35.5 / 36.7	27.4

Table 7: Ablation study on mixup parameter θ of extrinsic CFA. Motifs [43] is used in all ablation on VG [18].

Component	SGCIs		
	En-IN	En-EX	IMG
✓			
	✓		
		✓	
✓	✓	✓	
			✓

Table 8: Ablation study on each enhanced strategy in MCFA on the VG dataset [18]. En-IN: Utilize relation-conditioned entity clustering in intrinsic-CFA. En-EX: Employ the adaptive feature augmentation in extrinsic-CFA. IMG: Use the image-level augmentation.

adap} under the SGCIs setting with Motifs [43] in Table 7. When θ is too small, the query triplet has too much impact on the other triplets in the image of the context triplet, and when θ is too large, feature augmentation of the query triplet is not strong enough. Our adaptive mixup operation alleviates this by dynamically calibrating θ based on the semantic similarity between the query and context predicates. Such calibration facilitates the targeted enrichment of tail predicates using relevant contexts, while concurrently preventing feature distortion from less pertinent ones, ultimately enhancing robustness.

Effectiveness of Each Enhanced Strategy in MCFA. We verified the effectiveness of each enhanced strategy on the original CFA, as presented in Table 8. Key observations are as follows: 1) Employing relation-conditioned entity clustering effectively identifies more suitable entities, leading to an improvement in Recall while maintaining a comparable mean Recall. 2) The adaptive mixup operation enables tail instances to better leverage contextual information from head instances, thereby significantly boosting mean Recall. 3) The adoption of image-level augmentation can simultaneously enhance recall and mean recall, which proves the rationality of generated triplets. 4) Combining all strategies allows MCFA to achieve the best Mean performance.

5 Qualitative Analysis

Visualization of Reasonable Entities in Intrinsic-CFA. Fig. 7 shows some alternative entities for query triplets. Although the visual features of these candidate entities can differ significantly from the original, they remain reasonable

substitutions within the query triplet. For example, while `zebra` samples may vary considerably in color and texture from a `giraffe`, both are suitable because they share the common behavior of “eating plants”. Replacing a `giraffe` with a `zebra` in such instances introduces new visual information, thereby enriching the feature diversity associated with the `eating` predicate.

Visualization of Generated Triplets for Image-level Augmentation. Fig. 8 displays some generated triplets (*cf.*, Sec. 3.3), illustrating our method’s capability to generate diverse examples (*e.g.*, `handle-on` `back` `of-toilet`) and to utilize the original query triplet’s bounding box for their supervision.

6 Conclusion

In this paper, we revealed the drawbacks of existing rebalancing methods and discovered that the key challenge for unbiased SGG is to learn proper decision boundaries under the severe long-tailed predicate distribution. To address this, we proposed a model-agnostic MCFA framework to enrich the feature space of tail categories. It augments both intrinsic and extrinsic features of relation triplets from the feature-level and image-level. At the feature-level, a relation-conditioned entity clustering strategy was designed for intrinsic augmentation and an adaptive mix-up strategy for extrinsic augmentation, dynamically adjusting based on predicate similarity. For image-level augmentation, we devised a generative method leveraging powerful models like GLIGEN to create new visual appearances for triplets, thereby overcoming in-domain data limitations. Comprehensive experiments on the challenging VG and GQA datasets consistently demonstrated that MCFA’s effectiveness for unbiased SGG.

Data Availability All experiments are conducted on publicly available datasets; see the references cited.

References

- Chen C, Zhan Y, Yu B, Liu L, Luo Y, Du B (2022) Resistance training using prior bias: toward unbiased scene graph generation. In: AAAI, pp 212–220 [2](#), [9](#), [10](#)
- Chen L, Zhang H, Xiao J, He X, Pu S, Chang SF (2019) Counterfactual critic multi-agent training for scene graph generation. In: ICCV, pp 4613–4623 [1](#)
- Chen T, Yu W, Chen R, Lin L (2019) Knowledge-embedded routing network for scene graph generation. In: CVPR, pp 6163–6171 [1](#)
- Chen T, Kornblith S, Norouzi M, Hinton G (2020) A simple framework for contrastive learning of visual representations. In: ICML, pp 1597–1607 [8](#)
- Chiou MJ, Ding H, Yan H, Wang C, Zimmermann R, Feng J (2021) Recovering the unbiased scene graphs from the biased ones. In: ACM MM [9](#), [10](#)
- Chu P, Bian X, Liu S, Ling H (2020) Feature space augmentation for long-tailed data. In: ECCV, pp 694–710 [2](#), [4](#)
- Deng Y, Li Y, Zhang Y, Xiang X, Wang J, Chen J, Ma J (2022) Hierarchical memory learning for fine-grained scene graph generation. In: ECCV [9](#), [10](#)
- Desai A, Wu TY, Tripathi S, Vasconcelos N (2021) Learning of visual relations: The devil is in the tails. In: ICCV, pp 15404–15413 [4](#)
- DeVries T, Taylor GW (2017) Improved regularization of convolutional neural networks with cutout. arXiv [4](#)
- Dong X, Gan T, Song X, Wu J, Cheng Y, Nie L (2022) Stacked hybrid-attention and group collaborative learning for unbiased scene graph generation. In: CVPR, pp 19427–19436 [9](#), [10](#)
- Guo Y, Gao L, Wang X, Hu Y, Xu X, Lu X, Shen HT, Song J (2021) From general to specific: Informative scene graph generation via balance adjustment. In: ICCV, pp 16383–16392 [9](#), [10](#)
- Gupta A, Dollar P, Girshick R (2019) Lvvis: A dataset for large vocabulary instance segmentation. In: CVPR, pp 5356–5364 [5](#)
- Hou Z, Peng X, Qiao Y, Tao D (2020) Visual compositional learning for human-object interaction detection. In: ECCV, pp 584–600 [4](#)
- Hou Z, Yu B, Qiao Y, Peng X, Tao D (2021) Detecting human-object interaction via fabricated compositional learning. In: CVPR, pp 14646–14655 [4](#)
- Hudson DA, Manning CD (2019) Gqa: A new dataset for real-world visual reasoning and compositional question answering. In: CVPR, pp 6700–6709 [3](#), [10](#)
- Jeon J, Kim K, Yoon K, Park C (2024) Semantic diversity-aware prototype-based learning for unbiased scene graph generation. In: ECCV, Springer, pp 379–395 [9](#), [10](#)
- Kato K, Li Y, Gupta A (2018) Compositional learning for human object interaction. In: ECCV, pp 234–251 [4](#)
- Krishna R, Zhu Y, Groth O, Johnson J, Hata K, Kravitz J, Chen S, Kalantidis Y, Li LJ, Shamma DA, et al. (2017) Visual genome: Connecting language and vision using crowdsourced dense image annotations. IJCV [2](#), [3](#), [9](#), [11](#), [12](#), [16](#), [17](#), [18](#)
- Li L, Chen L, Huang Y, Zhang Z, Zhang S, Xiao J (2022) The devil is in the labels: Noisy label correction for robust scene graph generation. In: CVPR, pp 18869–18878 [1](#), [4](#), [9](#), [10](#)
- Li L, Chen L, Shi H, Zhang H, Yang Y, Liu W, Xiao J (2022) Nicest: Noisy label correction and training for robust scene graph generation. arXiv [4](#)
- Li L, Chen G, Xiao J, Yang Y, Wang C, Chen L (2023) Compositional feature augmentation for unbiased scene graph generation. In: ICCV, pp 21685–21695 [4](#), [7](#), [9](#), [10](#), [12](#)
- Li P, Li D, Li W, Gong S, Fu Y, Hospedales TM (2021) A simple feature augmentation for domain generalization. In: ICCV, pp 8886–8895 [4](#)
- Li R, Zhang S, Wan B, He X (2021) Bipartite graph network with adaptive message passing for unbiased scene graph generation. In: CVPR, pp 11109–11119 [1](#), [2](#), [4](#), [5](#), [9](#), [10](#)
- Li W, Zhang H, Bai Q, Zhao G, Jiang N, Yuan X (2022) Pndl: Predicate probability distribution based loss for unbiased scene graph generation. In: CVPR, pp 19447–19456 [2](#), [4](#), [9](#), [10](#)
- Li X, Chen L, Shao J, Xiao S, Zhang S, Xiao J (2022) Rethinking the evaluation of unbiased scene graph generation. In: BMVC [10](#), [14](#)
- Li Y, Liu H, Wu Q, Mu F, Yang J, Gao J, Li C, Lee YJ (2023) Gligen: Open-set grounded text-to-image generation. In: Proceedings of the IEEE/CVF conference on computer vision and pattern recognition, pp 22511–22521 [3](#), [8](#)
- Lin TY, Dollár P, Girshick R, He K, Hariharan B, Belongie S (2017) Feature pyramid networks for object detection. In: CVPR, pp 2117–2125 [10](#)
- Liu Z, Miao Z, Zhan X, Wang J, Gong B, Yu SX (2019) Large-scale long-tailed recognition in an open world. In: CVPR, pp

29. Lu C, Krishna R, Bernstein M, Fei-Fei L (2016) Visual relationship detection with language priors. In: ECCV, pp 852–869 1
30. Lu Y, Rai H, Chang J, Knyazev B, Yu G, Shekhar S, Taylor GW, Volkovs M (2021) Context-aware scene graph generation with seq2seq transformers. In: ICCV, pp 15931–15941 1
31. Lyu X, Gao L, Guo Y, Zhao Z, Huang H, Shen HT, Song J (2022) Fine-grained predicates learning for scene graph generation. In: CVPR 2, 4
32. Pennington J, Socher R, Manning CD (2014) Glove: Global vectors for word representation. In: EMNLP, pp 1532–1543 5
33. Radford A, Kim JW, Hallacy C, Ramesh A, Goh G, Agarwal S, Sastry G, Askell A, Mishkin P, Clark J, et al. (2021) Learning transferable visual models from natural language supervision. In: International conference on machine learning, PMLR, pp 8748–8763 8
34. Ren S, He K, Girshick R, Sun J (2015) Faster r-cnn: Towards real-time object detection with region proposal networks. In: NeurIPS, pp 91–99 4
35. Tang K, Zhang H, Wu B, Luo W, Liu W (2019) Learning to compose dynamic tree structures for visual contexts. In: CVPR, pp 6619–6628 1, 4, 5, 9, 10
36. Tang K, Niu Y, Huang J, Shi J, Zhang H (2020) Unbiased scene graph generation from biased training. In: CVPR, pp 3716–3725 1, 4, 9, 10, 16
37. Vaswani A, Shazeer N, Parmar N, Uszkoreit J, Jones L, Gomez AN, Kaiser Ł, Polosukhin I (2017) Attention is all you need 9, 10
38. Vigneswaran R, Law MT, Balasubramanian VN, Tapaswi M (2021) Feature generation for long-tail classification. In: ICVGIP, pp 1–9 2
39. Wei M, Yuan C, Yue X, Zhong K (2020) Hose-net: Higher order structure embedded network for scene graph generation. In: ACM MM, pp 1846–1854 14
40. Xu D, Zhu Y, Choy CB, Fei-Fei L (2017) Scene graph generation by iterative message passing. In: CVPR, pp 5410–5419 8, 9
41. Yan S, Shen C, Jin Z, Huang J, Jiang R, Chen Y, Hua XS (2020) PcpL: Predicate-correlation perception learning for unbiased scene graph generation. In: ACM MM, pp 265–273 2, 4, 9, 10
42. Yu J, Chai Y, Hu Y, Wu Q (2021) Cogtree: Cognition tree loss for unbiased scene graph generation. In: IJCAI 4, 5, 9, 10
43. Zellers R, Yatskar M, Thomson S, Choi Y (2018) Neural motifs: Scene graph parsing with global context. In: CVPR, pp 5831–5840 1, 4, 5, 9, 10, 11, 12, 16, 17
44. Zhang A, Yao Y, Chen Q, Ji W, Liu Z, Sun M, Chua TS (2022) Fine-grained scene graph generation with data transfer. In: ECCV 9, 10
45. Zhang H, Kyaw Z, Chang SF, Chua TS (2017) Visual translation embedding network for visual relation detection. In: CVPR, pp 5532–5540 1
46. Zhong Z, Zheng L, Kang G, Li S, Yang Y (2020) Random erasing data augmentation. In: AAAI, pp 13001–13008 4

Appendix

This appendix is organized as follows:

- The hierarchical clustering process and results mentioned in Sec. 3.2.1 are shown in Sec. A.
- A more detailed discussion of prior knowledge mentioned in Sec. 4.2 is shown in Sec. B.
- More experimental comparisons and analyses are shown in Sec. C

A Relation-Conditioned Entity Clustering

As mentioned in Sec. 3.2.1, we use relation-conditioned entity clustering to mine the replaceable entity categories. The specific implementation is detailed in Algorithm 1, which involves two main hierarchical clustering stages: first for predicates, and subsequently for entities, conditioned on these predicate clusters. Both stages utilize a similar iterative merging procedure.

The cluster similarity functions, Sim_P for predicates and Sim_E for entities, are the weighted sum of pattern, context, and semantic similarities. In practice, we treat clusters as a collection of multiple entity categories, and the pattern and context similarity can be transferred directly from class-level to cluster-level. For semantic similarity, we take the mean similarity for the categories between clusters.

After initializing the variables, the predicate and entity clustering stages share a similar logic in each iteration. First, we select the two most similar clusters (SELECT_MAX) based on similarity matrix (A_{sim}^P for predicates or A_{sim}^E for entities) and size of cluster (l^P or l^E). Given that the distribution of different relation triplets in datasets is often highly imbalanced, we follow [39] to employ the cluster size as a penalty term. This aims to prevent categories (whether predicate or entity) with a large proportion of samples from unduly dominating the clustering process. Subsequently, we merge the predicate or entity categories in cluster s_j^P or s_j^E into s_i^P or s_i^E (MERGE), remove cluster s_j^P / s_j^E , and update the corresponding cluster size. Since the merged cluster has changed, we recalculate the similarity of other clusters to it and then update A_{sim}^P / A_{sim}^E (UPDATE). The above steps are repeated until the number of clusters is equal to K^P for predicates or K^E for entities.

The predicate clustering result and entity clustering results are shown in Fig. 9 and Fig. 10, respectively. Obviously, some predicate and entity categories that share common pattern are grouped into the same cluster, e.g., lying on and laying on (predicates), and dog and cat (entities, grouped within relevant predicate cluster contexts).

B Component Prior Knowledge

As discussed in prior SGG works [25], the statistic prior of the predicate distribution under a given condition can improve the mR@K performance of the unbiased SGG. In the inference phase, we calculate statistic component prior $b_{s,o,r}$, and add it to the predicted logits to predict predicate category:

$$b_{s,o,r} = -\log \frac{count_{s,o,r}}{\sum_{i=1}^H count_{s,o,i}}, \quad (19)$$

where H is the number of predicate categories. As for the prior “Triplet”, “Subject”, and “Object”, $count_{s,o,r}$ is the amount of the triplets whose predicate category is r in the training set given subject-object pair, subject, and object respectively.

Algorithm 1: Relation-Conditioned Entity Clustering

Input: Predicate category set $C_P = \{c_{p_i} \mid i = 1, 2, \dots, N_p\}$;
Entity category set $C_E = \{c_{e_i} \mid i = 1, 2, \dots, N_e\}$;
Predicate cluster similarity function Sim_P ;
Entity cluster similarity function Sim_E ;
Target number of predicate clusters K_p ;
Target number of entity clusters K_e within each predicate cluster;
Output: Set of all predicate clusters $\mathcal{S}^p = \{s_i^p \mid i = 1, 2, \dots, K_p\}$
Set of all entity clusters $\mathcal{S}^e = \{s_i^e \mid i = 1, 2, \dots, K_e\}$ within each predicate cluster s_i^p

```

/* --- Step 1: Predicate Clustering --- */  

/* Initialize each predicate category as a cluster */  

for  $i = 1, 2, \dots, N_p$  do  

   $s_i^p = \{c_{p_i}\}$   

/* Initialize the size of each cluster  $l_i^p$  and the similarity matrix  $A_{sim}^p$  */  

for  $i = 1, 2, \dots, N_p$  do  

   $l_i^p = 1$   

  for  $j = 1, 2, \dots, N_p$  do  

     $A_{sim}^p(i, j) = Sim_P(s_i^p, s_j^p)$   

     $A_{sim}^p(j, i) = A_{sim}^p(i, j)$   

/* Merge the two most similar predicate cluster until the number of clusters is smaller  

than  $K_p$  */  

while  $LEN(\mathcal{S}^p) > K_p$  do  

   $s_i^p, s_j^p = \text{SELECT\_MAX}(A_{sim}^p(i, j) / (l_i^p + l_j^p))$   

   $s_i^p = \text{MERGE}(s_i^p, s_j^p)$   

   $\mathcal{S}^p = \mathcal{S}^p - s_j^p$   

   $l_i^p = l_i^p + l_j^p + 1$   

   $\text{UPDATE}(A_{sim}^p)$   

/* --- Step 2: Predicate Merging --- */  

for each predicate cluster  $s_i^p \in \mathcal{S}^p$  do  

  for  $c_{e_i} \in C_E$  do  

    if  $c_{e_i}$  is in the same triplet category with  $c_{p_i} \in s_i^p$  then  

       $C_E^{s_i^p} \leftarrow c_{e_i}$   

/* --- Step 3: Entity Clustering within each Predicate Cluster --- */  

for each predicate cluster  $s_i^p \in \mathcal{S}^p$  do  

  /* Initialize each entity category as a cluster */  

  for  $i = 1, 2, \dots, |C_E^{s_i^p}|$  do  

     $s_i^e = \{c_{e_i}\}$   

  /* Initialize the size of each cluster  $l_i^e$  and the similarity matrix  $A_{sim}^e$  */  

  for  $i = 1, 2, \dots, N_e$  do  

     $l_i^e = 1$   

    for  $j = 1, 2, \dots, N_e$  do  

       $A_{sim}^e(i, j) = Sim_E(s_i^e, s_j^e)$   

       $A_{sim}^e(j, i) = A_{sim}^e(i, j)$   

/* Merge the two most similar entity cluster until the number of clusters is smaller  

than  $K_e$  */  

while  $LEN(\mathcal{S}^e) > K_e$  do  

   $s_i^e, s_j^e = \text{SELECT\_MAX}(A_{sim}^e(i, j) / (l_i^e + l_j^e))$   

   $s_i^e = \text{MERGE}(s_i^e, s_j^e)$   

   $\mathcal{S}^e = \mathcal{S}^e - s_j^e$   

   $l_i^e = l_i^e + l_j^e + 1$   

   $\text{UPDATE}(A_{sim}^e)$   

return  $\mathcal{S}^e$  for each predicate cluster  $s_i^p$ ;

```

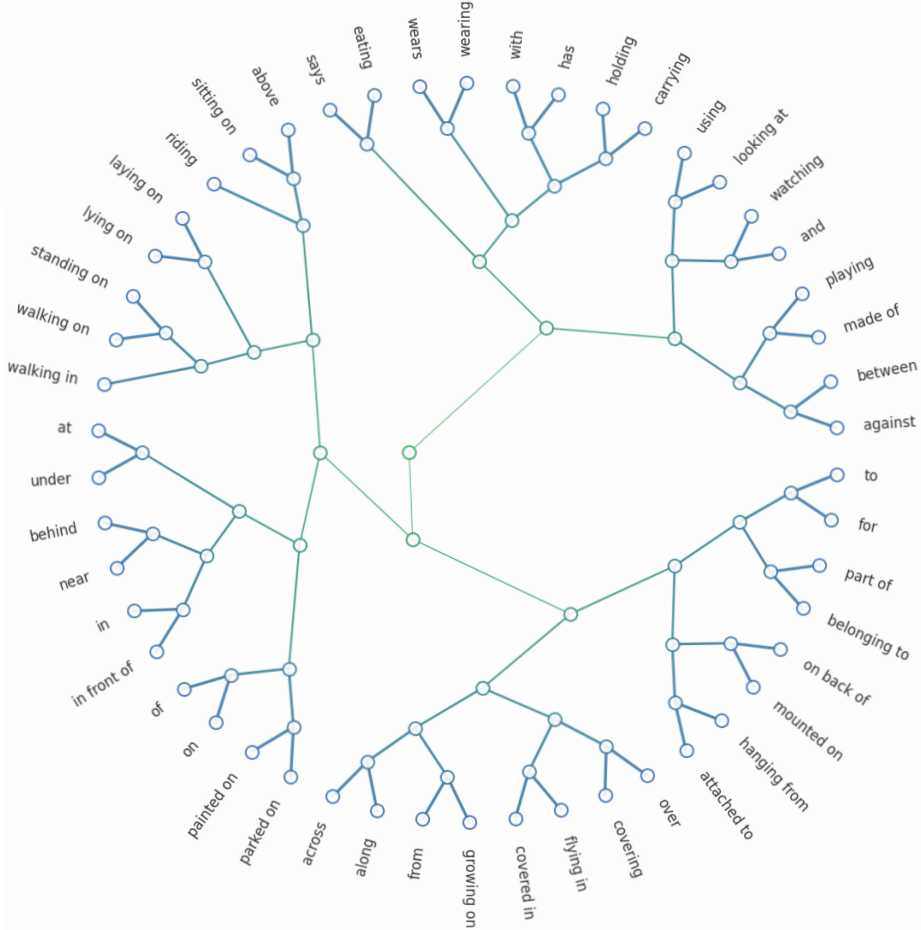


Fig. 9: The results of relation clustering on VG [18].

Strategy	PredCls		
	mR@50 / 100	R@50 / 100	Mean
Motifs [43]	16.5 / 17.8	65.6 / 67.2	41.8
+Reweighting [36]	30.8 \uparrow 14.3 / 34.5 \uparrow 16.7	36.1 / 40.4	35.5
+Resample [36]	18.5 \uparrow 2.0 / 20.0 \uparrow 2.2	64.6 / 66.7	42.5
+MCFA	35.8 \uparrow 18.7 / 38.3 \uparrow 20.5	54.3 / 56.8	46.3

Table 9: Performance (%) of re-balancing strategies and MCFA on VG [18].

C Extra Comparisons and Analyses

C.1 Comparison with Re-balancing Methods.

To demonstrate the superiority of MCFA compared with the prevalent re-balancing methods (*i.e.*, reweight and resample) [36], we conducted the three strategies on the baseline Motifs [43]. The results under the PredCls setting are reported in Table 9. From the results, we can observe: 1) The Motifs baseline can achieve the best R@K. However, the high R@K is mainly due to the frequency bias of the dataset [36], and they suffer severe drops in tail predicates. 2) The reweight method achieves better performance at mR@K, but it also sacrifices the performance of head predicates excessively, resulting in a low Mean. 3) The resample method keeps R@K high, but the improvement of mR@K is slight. The reason is that those decision boundaries may still be biased toward the head. 4) MCFA achieves the highest mR@K and maintains

high R@K, *i.e.*, it achieves the best trade-off over different predicate categories (highest performance on Mean).

C.2 Comparison over All Predicates

To further demonstrate the performance of each predicate, we displayed the predicate distribution of the training set in the VG dataset [18] and the performance of Motifs [43] and Motifs+MCFA on R@100 for each predicate category in Fig. 11. Obviously, our approach slightly compromises the performance of the head predicates (*e.g.*, wearing), but greatly improves the tail predicates (*e.g.*, flying in). This proves the superiority of our method in considering the performance of all predicates.

C.3 Qualitative Results.

Figure 12 shows some qualitative results generated by Motifs [43] and Motifs+MCFA under PredCls setting. We can observe that MCFA can not only predict more accurate predicates (*e.g.*, on vs. parked on and on vs. walking on), but also more fine-grained and informative predicates (*e.g.*, holding vs. using).

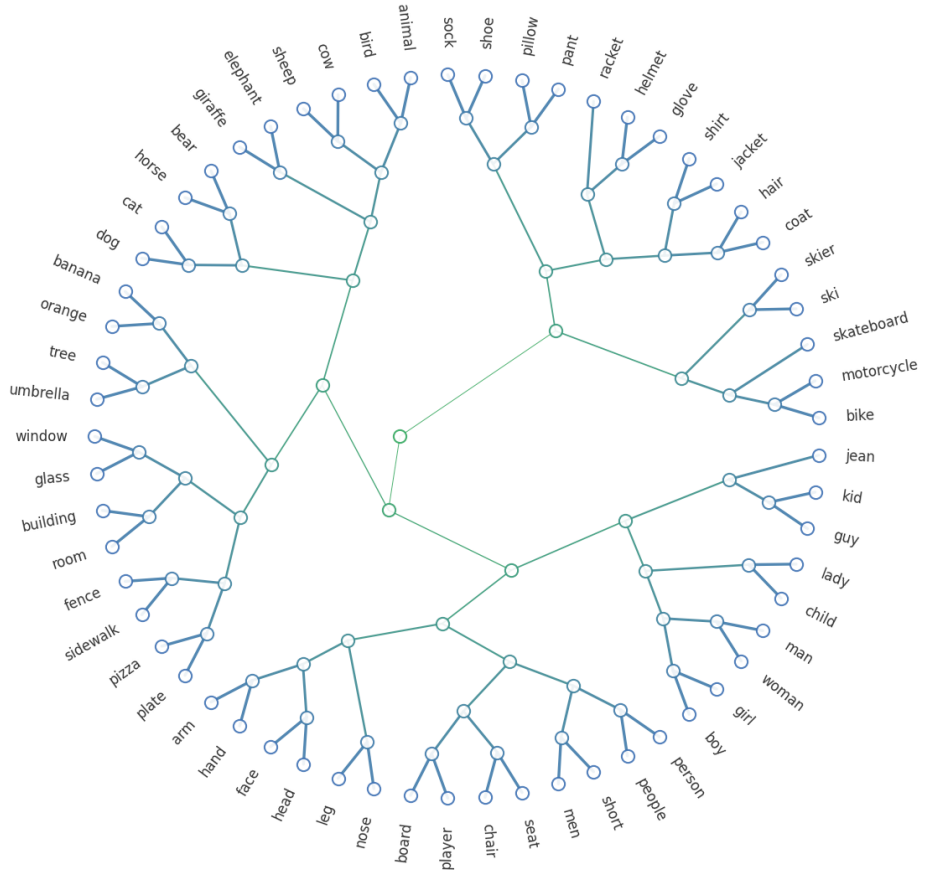


Fig. 10: The results of entity clustering on VG [18].

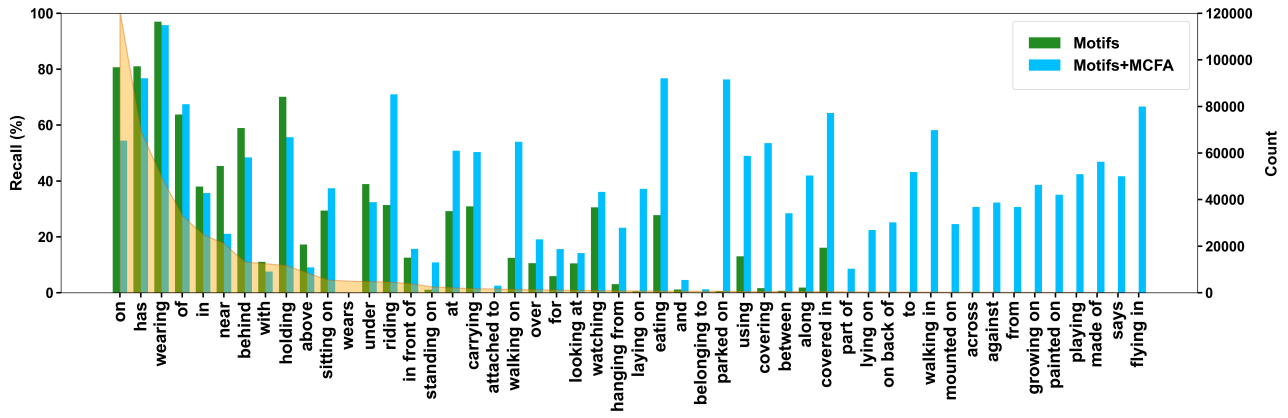


Fig. 11: Performance(%) comparison between Motifs [43] and Motifs+CFA over all predicates on test set of VG [18]. The orange area denotes the predicate distribution of training set.

C.4 Quality of Compositional Features.

We visualized the t-SNE distributions of features (from the previous layer of classification) in Fig. 13, demonstrating that our MCFA enhances the distinctiveness of tail predicates in feature space, *i.e.*, it aids in finding suitable decision boundaries and does not harm to training, resulting in improved performance.

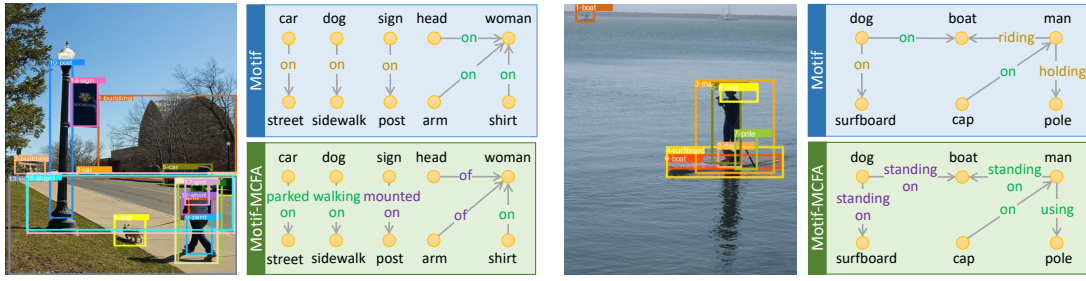


Fig. 12: The results of scene graphs generated by Motifs (blue) and Motifs-MCFA (green) on VG [18]. **Green** predicates are correct (*i.e.*, match GT), **brown** predicates are acceptable (*i.e.*, does not match GT but still reasonable), and **purple** predicates are more informative (*i.e.*, does not match GT and more reasonable).

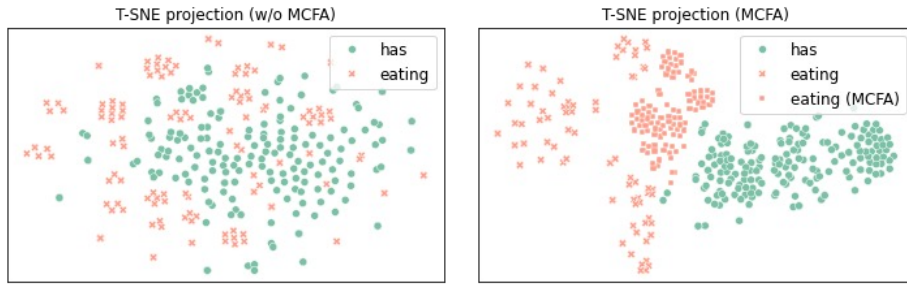


Fig. 13: The t-SNE visualization of randomly sampled instances of two predicates on the feature space before and after MCFA.